LAWRENCE
LIVERMORE
NATIONAL
LABORATORY

UCRL-JRNL-223935

Accurate labeling of the light-actinide O4,5 ionization edges

K. Moore, G. van der Laan

August 23, 2006

Ultramicroscopy

Elsevier Editorial System(tm) for Ultramicroscopy

Manuscript Draft

Manuscript Number:

Title: Accurate labeling of the light-actinide O4,5 edges

Article Type: Short Communication

Keywords: EELS, TEM, actinide, and absorption

Corresponding Author: Dr. Kevin Moore, PhD

Corresponding Author's Institution: Lawrence Livermore National Laboratory

First Author: Kevin Moore, PhD

Order of Authors: Kevin Moore, PhD; Gerrit van der Laan, PhD

Abstract: In this short article the accurate labeling of the O4,5 edges of the light actinides is addressed. The O4 and O5 edges are both contained in what is termed the 'giant resonance' and the smaller 'pre-peak' that is observed is a consequence of first-order perturbation by the 5d spin-orbit interaction. Thus, the small pre-peak in the actinide 5d → 5f transition should not be labeled the O5 peak, but rather the ΔS=1 peak.

*** Suggested Referees**

Professor Gianluigi Botton
http://mse.mcmaster.ca/faculty/botton/
Associate Professor
Materials Science and Engineering,
McMaster University
1280 Main Street West, Hamilton
Ontario, Canada L8S 4L7
e-mail: gbotton@mcmaster.ca

Professor Peter Rez
http://www.public.asu.edu/~atppr/
Department of Physics and Astronomy
Arizona State University
PO Box 871504
Tempe, AZ 85287-1504 USA
Office Location: PSA 336
Office Telephone: 602-965-6449
Email address: Peter.Rez@asu.edu

Accurate labeling of the light-actinide $O_{4,5}$ edges

Kevin T. Moore[1] and Gerrit van der Laan[2]

[1]*Chemistry and Materials Science Directorate, Lawrence Livermore National Laboratory, Livermore, California 94550, USA.*

[2]*Magnetic Spectroscopy Group, Daresbury Laboratory, Warrington WA4 4AD, UK.*

In this short article the accurate labeling of the $O_{4,5}$ edges of the light actinides is addressed. The O_4 and O_5 edges are both contained in what is termed the 'giant resonance' and the smaller 'pre-peak' that is observed is a consequence of first-order perturbation by the 5*d* spin-orbit interaction. Thus, the small pre-peak in the actinide $5d \rightarrow 5f$ transition should not be labeled the O_5 peak, but rather the $\Delta S=1$ peak.

PACS: 79.20.Uv, 71.10.-w, 71.70.Ej, 71.70.Gm
Keywords: EELS, TEM, actinide, and absorption.

Contact Author
Tel: 925-422-9741
Fax: 925-422-6892
Email: moore78@llnl.gov

Actinide materials of are great interest presently to the physics and chemistry communities due to the intriguing and unique physical properties they exhibit as a result of the complicated electronic structure of the 5*f* states. In order to investigate these states, x-ray absorption spectroscopy (XAS) and electron energy-loss spectroscopy (EELS) are often employed, particularly transitions from *d* core states as this directly probes the *f* states. Since these transitions are of great importance to understanding actinide materials, it is imperative that we fully understand the $d \rightarrow f$ transitions and label them accurately. Here, the accurate labeling of the $O_{4,5}$ edges for the light actinides is addressed due to noticeable confusion in the literature and in private communications. The correct labeling of the edges will be presented along with analysis of calculated spectra.

Experimental

EELS spectra were collected in standard fashion using a Philips CM300 field-emission-gun transmission electron microscope and Gatan image filter with a 2k x 2k CCD chip. For full details of sample preparation and experimental parameters see references 1 and 2.

The $O_{4,5}$ EELS edges of Th, U, and Pu metal are shown in Figure 1 as solid grey, where the background has been removed using an inverse power law extrapolation. First consider Th. There is a small peak at ~88 eV and a second larger peak at ~101 eV. Often, the small peak at 88 eV is labeled the O_5 edge and the large peak at 101 eV is labeled the O_4 edge. The same labeling scheme is frequently used for U, which again shows a smaller initial peak followed by a larger and broader peak. In each case, this is incorrect. In reality, the dipole allowed transitions in an *LS* coupled final state are both contained in the larger second peak, which is frequently referred to as the 'giant resonance'. The smaller peak at lower energy is a dipole-forbidden transition, produced by the finite spin-orbit interaction. The latter is small compared to the 5*d*,5*f* Coulomb and exchange interaction, which generates energy splittings around 20 eV. This origin of the pre-peak(s) has in fact been explained in detail for the rare earths [3-5] and the actinides [6].

Core-level photoemission data reported that the $5d_{3/2}$ and $5d_{5/2}$ sublevels are separated by 7.1, 8.6, and 12.4 eV, for Th, U and Pu, respectively [7]. This agrees reasonably well with atomic Hartree-Fock calculations for the *5d* spin-orbit interaction, which give splittings of 6.7, 7.9 and 9.3 eV for f^1, f^3 and f^5, respectively. In the case of Th and U the separation between the pre-peak and the giant resonance is almost double the separation of the initial *d* states reported from photoemission [7]. To look at this in a more quantitative manner, the second derivative of each $O_{4,5}$ EELS edge can be calculated and compared to the edge itself. The second derivative of each edge is shown in Figure 1 as an overlayed black line, and when this is done it seems that the O_4 and O_5 edges are indeed both contained in the giant resonance. For Th there are two peaks in the second derivative, one for the small initial pre-peak and one for the giant resonance. In this case, the $5d_{3/2}$ and $5d_{5/2}$ initial states are close enough in energy that they are not resolved as separate in the giant resonance, partly due to the 2 eV lifetime broadening in actinide materials [8]. For U, the second derivative again shows two large peaks due to the pre-peak and the giant resonance. However, there is now a shoulder on the lower energy side of the giant resonance, which is located at approximately 105 eV. The difference between the inflection and the peak of the giant resonance is about 7 eV. This matches the 8.6 eV splitting between the initial $d_{3/2}$ and $d_{5/2}$ states of U reported by core-level photoemission quite well [7]. In the case of Pu the second derivative shows two large peaks that both emanate from the giant resonance alone, one located at about 122 eV and the other located at about 110 eV. These are separated by 12 eV, which is very close to the 12.4 eV spin-orbit splitting of the $5d_{3/2}$ and $5d_{5/2}$ initial states of Pu reported by core-level photoemission [7].

The idea that the $5d_{3/2} \rightarrow 5f$ and $5d_{5/2} \rightarrow 5f$ dipole allowed transitions are both contained in the giant resonance can be further considered by comparison of the U and UO_2 EELS spectra. The $O_{4,5}$ EELS edge of UO_2 is shown in Figure 2 as before with the spectra in gray and the second derivative overlayed as a black line. Notice that while the pre-peak is essentially unchanged from the metal, the inflection on the giant resonance has become more pronounced. This clearly shows that as the bonding environment changes it is the

inflection that changes and not the pre-peak. Thus, while it is tempting to ascribe the pre-peak and giant resonance as the O_5 and O_4 edges, respectively, this is incorrect. The electrostatic interactions are at least twice as large and these will completely mix the spin-orbit split peaks. The mixed spin-orbit split O_5 and O_4 peaks are both contained in the giant resonance and the small pre-peak is a consequence of first-order perturbation by the 5*d* spin-orbit interaction, as we will show below in the theoretical section.

Theoretical

In order to investigate the peak assignment of the $O_{4,5}$ edge theoretically we performed atomic multiplet calculations using the relativistic Hartree-Fock code of Cowan [9], where we omitted the decay channels. Although it is possible to include the decay process to reproduce the experimentally observed broadening and asymmetry of the spectra lines, it only has a small effect on the assignment of the core hole excited states. Moreover, the precise strength of the different decay channels is difficult to assess and its investigation is still ongoing [10]. Figure 3 shows the atomic calculations for the electric-dipole transitions $5d^{10}5f^{n} \rightarrow 5d^{9}5f^{n+1}$ with (black curves) and without (red curves) 5*d* core spin-orbit interaction for the ground state configurations with $n = 0$, 1, 2 and 5. The calculational method and parameter values are similar to those in Ref. [11], in which comparable results are shown. It is immediately clear from the spectra in Figure 3 that if the 5*d* spin-orbit interaction is switched off, the pre-peak structure vanishes. At the same time, the peaks within the main structure squeeze in a bit, however their intensities remain much the same.

With increasing atomic number *Z* both the 5*d* spin-orbit and 5*d*-5*f* electrostatic interaction increase, so that the ratio of these two interactions remains approximately the same. This means that along the 5*f* series the final state maintains a similar kind of intermediate coupling. In the case of the shallow $O_{4,5}$ edge this is closer to *LS* than to *jj* coupling. The XAS and EELS spectra can be calculated using the selection rules between initial and final state with quantum numbers *LSJ* and *L'S'J'*, respectively. For electric-dipole transitions the selection rules are $\Delta J = J - J' = -1,0,1$, with the restriction that $J' = J = 0$ is not allowed. In *LS* coupled basis we have, in addition to the selection rule on *J*, the following selection rules: $\Delta S = S - S' = 0$ and $\Delta L = L - L' = -1,0,1$, with $L' = L = 0$ not allowed [14].

We start off with the analysis of the spectrum for $5f^0$, which provides insight due to its simplicity. The ground state $5f^0$ is $^1S_0$ (i.e. L=S=J=0). The final state $5d^9 5f^1$ has L = 1, 2, 3, 4, 5 and S = 0, 1, among which only the ^3D, ^3P and ^1P states contain a J = 1 level. From the ground state $^1S_0$, only transition to the final state $^1P_1$ is allowed in *LS* coupled basis. When the 5*d* spin-orbit interaction is switched on, *L* and *S* cease to be good quantum numbers, and levels of the same *J* value will mix, so that $^1P_1$ mixes with $^3D_1$ and $^3P_1$. This mixing is described by the final state Hamiltonian for J = 1, which is a 3x3 matrix, where the diagonal elements contain the electrostatic interactions and the non-diagonal elements contain the spin-orbit interaction. Matrix diagonalization gives the required eigenvalues and eigenstates. The results are shown in Table I using the atomic

values of the spin-orbit and Slater parameters (see caption for values). Table II gives the results when the spin-orbit interaction is switched off. It is seen that the triplet states ($^3P_1$ and $^3D_1$) are at the low energy site and the singlet state ($^1P_1$) is at the high energy site, which is due to the strong 5*d*,5*f* exchange interaction. For each final state the tables show the $^3P_1$, $^3D_1$ and $^1P_1$ characters (i.e. the square of the wavefunction coefficients). The spectral intensity of each peak is given by the amount of $^1P_1$ character in the final state. In *LS* coupling where the 5*d* spin-orbit interaction is zero, the final state $^1P_1$ is pure and this peak has 100% of the intensity (c.f. Table II). If the core spin-orbit interaction is gradually switched on, we move from *LS* coupling to intermediate coupling, and the intensities of the other two peaks, which are labeled "$^3P_1$" and "$^3D_1$" according to their main character, gain some intensity due to the small amount of $^1P_1$ character that is mixed in (see Table I). We can conclude that the states corresponding to the pre-peaks have mainly triplet character, while the "$^1P_1$" state representing the giant resonance has mainly singlet character.

The above can also be understood from a perturbation type of approach. In the $O_{4,5}$ edge the electrostatic interactions are much larger than the spin-orbit coupling, so that the latter can be considered as a perturbation. First-order perturbation theory gives then an energy separation between the triplet and singlet states of $\Delta E = \sqrt{\left(\Delta E_{electrostatic}\right)^2 + \left(\Delta E_{spin\text{-}orbit}\right)^2}$ and a relative intensity for the "forbidden" triplet states of $I_{\text{triplet}} / I_{\text{singlet}} = \left(\Delta E_{\text{spin-orbit}}\right)^2 / \left(2\Delta E_{\text{electrostatic}}\right)^2$, where $\Delta E_{electrostatic}$ and $\Delta E_{spin\text{-}orbit}$ are the effective splitting due to the electrostatic interactions and the spin-orbit interaction, respectively. Comparing this to the values given in Table I, which were obtained from exact matrix diagonalization, shows that this simple perturbation model holds reasonably well. Therefore, the relative intensity of the pre-peak structure is a sensitive measure for the strength of the 5*d* core spin-orbit interaction relative to the *5d,5f* electrostatic interaction.

The picture for the other light elements f^n is similar but becomes rapidly more complicated with increasing *n*. The main peaks in the spectrum are due to the allowed transitions $\Delta S = 0$, $\Delta L = -1,0,1$. For a ground state $f^1(^2F_{5/2})$ the allowed transitions to a final state in *LS* coupled basis are $^2D_{J'}$, $^2F_{J'}$ and $^2G_{J'}$, where *J'* = 3/2, 5/2 and 7/2. The matrices for *J'* = 3/2, 5/2 and 7/2 have a dimension of 15, 19 and 19, respectively, giving a total of 53 final states. The small 5*d* spin-orbit interaction allows "forbidden" transitions with $\Delta S = 1$ to final states with quartet spin (*S*=3/2) which are at lower energy due to the 5*d*,5*f* exchange energy. The splitting within the main peak is due to both Coulomb interaction and spin-orbit interaction and these cannot be separated.

For $f^2(^3H_4)$ the dipole allowed transition are to $^3G_{J'}$, $^3H_{J'}$ and $^3I_{J'}$ states with *J'* = 3, 4 and 5. In intermediate coupling, the ground state is a mixture of different *LS* states, namely 88% $^3H_4$, 1% $^3F_4$, and 11% $^1G_4$. This means that the simple model based on ^1P parentage already begins to break down. Analysis of the pre-peak structure shows that it contains a mixture of mainly triplet and quintet spin states. Likewise, for the $f^5(^6H_{5/2})$ spectrum (where the matrices for *J'* = 3/2, 5/2 and 7/2 have a dimension of 246, 329 and 371, respectively) the pre-peak is a mixture of different spin states, however the average spin

of the pre-peak is higher than that of the giant resonance. In all cases the pre-peak intensity increases with the size of the 5*d* spin-orbit interaction relative to the electrostatic interactions. Since the spin-orbit interaction of the 5*d* is about tenfold larger than that of the 5*f* shell, the latter has only minor influence. Nevertheless, the angular quantum number for the 5*f* states (j=7/2 or 5/2) strongly influences the precise spectral shape of the pre-peak structure and the position of the giant resonance.

For less than half-filled shell, the "forbidden" states of high spin at lower energies are always present. The reason for this is that for a ground state $5f^n$ with maximum spin S, the maximum spin for the final state $5d^9 5f^{n+1}$ is S+1 for $n \leq 6$ and S for $n \geq 7$ (c.f. Figure 3 in Ref. [12]). The energy separation between the states with different spins is given by the exchange interaction. A necessary requirement of a *sharp* pre-peak is that its decay lifetime is long: A high spin state has the advantage that there are no, or only a few, states with the same S into which it can decay. The excited state is then sometimes called "double forbidden". Complications in the *LS* picture arise from the fact that the ground state is strongly mixed, e.g. $5f^3$ has 84% S=4 and 16% S=2, and $5f^5$ has 67% S=6, 27% S=4 [13]. This increased mixing of the spin states causes a decrease in energy separation between the pre-peak and giant resonance with increasing Z. Furthermore, the simple *LS* coupling model starts to break down because the ^1P parentage cannot be traced to a single level [5].

As a further check we also determined the core spin-orbit character of each peak. The *jj*-*LS* transformation matrix [14] enables us to write the three *LS* states as linear combination of $d_{5/2}f_{7/2}$, $d_{5/2}f_{5/2}$ and $d_{3/2}f_{5/2}$ states. Adding together the contributions of $f_{7/2}$ and $f_{5/2}$, the amounts of core hole $d_{5/2}$ and $d_{3/2}$ character for excitation from the ground state $5f^0$ are given in Table I and II. It is seen that the "$^3D_1$" and "$^1P_1$" peaks have strongly mixed j character (~60% : ~40%). This is of course not surprising since it is the electrostatic interaction, and not the spin-orbit, that is dominant. This clearly shows that for accurate labeling, the core hole angular momentum j is unsuitable. The "$^3P_1$" peak is rather pure but has negligible intensity.

For the actinide $N_{4,5}$ ($4d \rightarrow 5f$) edge the situation is completely opposite: the spin-orbit interaction is dominant over the electrostatic interaction, as seen in Table III. The $4d_{5/2}$ and $4d_{3/2}$ peaks, or 'white lines', are well separated by the large core spin-orbit splitting that is on the order of 40 eV and considerably larger than the electrostatic interaction. In this case, j is a good quantum number, whilst the *LS* states are strongly mixed. The branching ratio of the white lines $d_{5/2}/(d_{5/2} + d_{3/2}) = 0.592$, which is close to the statistical ratio of 0.6. Hence the actinide $N_{4,5}$ edge is ideally suited for sum rule analysis, which requires a negligible *jj* mixing [15].

The experimentally observed splitting in the $O_{4,5}$ giant resonance (Figures 1 and 2) should therefore not be ascribed to the core spin-orbit splitting as seemed by comparison to the core-level photoemission [7], but rather to the energy splitting of the three dipole allowed transitions (ΔL = -1,0,1 and ΔS = 0). The $5d_{3/2} \rightarrow 5f$ and $5d_{5/2} \rightarrow 5f$ transitions are completely mixed into these states and, therefore, are both indeed contained in the giant resonance, but are entirely unresolvable.

The behavior of the actinide $O_{4,5}$ (5*d*) edges [11] can be compared to that of the rare earth $N_{4,5}$ (4*d*) edges [16,17] and the 3*d* transition metal $M_{2,3}$ (3*p*) edges [18]. In all these cases the core spin-orbit interaction is much smaller than the core-valence electrostatic interactions. The 4*f* metals show a pre-peak structure that is rather insensitive to the local environment [3-5]. The 3*d* metals show a pre-peak structure that is strongly dependent on the crystal field and hybridization [16]. Since the 5*f* localization is between those of 4*f* and 3*d*, we might expect for the actinides to show only a mild dependence on the environment.

Conclusions

An assignment of the actinide $O_{4,5}$ edge can be made on the basis of final state *LS* coupling, and in doing so it can be shown that the dipole allowed transitions are contained within the giant resonance. The giant resonance splits into three transitions that are dipole allowed: $\Delta S = 0$ and $\Delta L = -1,0,1$ ($\Delta L = 1$ for ^1S ground state), where *S* and *L* are the spin and orbital quantum numbers of the ground state. The 5*d* spin-orbit interaction can be considered as a perturbation giving raise to a pre-peak structure containing $\Delta S = 1$ states. These states have a lower energy than the $\Delta S = 0$ states with a separation determined by the strong 5*d*,5*f* exchange interaction. Although this simple picture begins to break down for $n>1$, because the ground state and final states are strongly mixed, a global assignment can still be made on basis of the spin states. Although atomic calculations are a simplification in the case of solids, they explain the trend along the series in the actinides rather well and show that the pre-peak observed in the $O_{4,5}$ edge is a dipole "forbidden" transition.

Acknowledgements

Special thanks to the Institute for Transuranium research for producing the UO_2 single crystals used for EELS measurements. This work was performed under the auspices of the U.S. Department of Energy by University of California Lawrence Livermore National Laboratory under contract number W-7405-Eng-48.

References

1. K.T. Moore, M.A. Wall, A.J. Schwartz, B.W. Chung, S.A. Morton, J.G. Tobin, S. Lazar, F.D. Tichelaar, H.W. Zandbergen, P. Söderlind, and G. van der Laan, *Philos. Mag.* **84**, 1039 (2004).
2. K.T. Moore, G. van der Laan, R.G. Haire, M.A Wall, and A.J. Schwartz, *Phys. Rev. B* **73**, 033109 (2006).
3. J.L. Dehmer A.F. Starace, U. Fano, J. Sugar, and J.W. Cooper, *Phys. Rev. Lett.* **26**, 1521 (1971).
4. A. F. Starace, *Phys. Rev. B* **5**, 1773 (1972).
5. J. Sugar, *Phys. Rev. B* **5**, 1785 (1972).
6. K.T. Moore, M.A. Wall, A.J. Schwartz, B.W. Chung, D.K. Shuh, Schulze, and J.G Tobin, *Phys. Rev. Lett.* **90**, 196404 (2003).

7. R. Baptist D. Courteix, J. Chayrouse, and L. Heintz, *J. Phys. F* **12**, 2103 (1982).
8. G. Kalkowski G. Kaindl, W.D Brewer, and W. Krone, *Phys. Rev. B* **35**, 2667 (1987).
9. R. D. Cowan, *J. Opt. Soc. Am.* **58**, 808 (1968).
10. H. Ogasawara and A. Kotani, *J. Synchrotron Rad.* **8**, 220 (2001).
11. H. Ogasawara, A. Kotani, and B.T. Thole, *Phys. Rev. B* **44**, 2169 (1991).
12. B.T. Thole and G. van der Laan, *Phys. Rev. B* **38**, 3158 (1988).
13. F. Gerken and J. Schmidt-May, *J. Phys. F. Met. Phys.* **13**, 1571 (1983).
14. G. van der Laan, *Lect. Notes Phys*. **697**, 143 (2006).
15. G. van der Laan, K.T. Moore, J.G. Tobin, B.W. Chung, M.A. Wall, and A.J. Schwatz, *Phys. Rev. Lett.* **93**, 097401 (2004).
16. H. Ogasawara and A. Kotani, *J. Phys. Soc. Jpn*. **64**, 1394 (1995).
17. K. Starke, E. Navas, E. Arenholz, Z. Hu, L. Baumgarten, G. van der Laan, C.T. Chen, and G. Kaindl, *Phys. Rev. B* **55**, 2672 (1997).
18. G. van der Laan, *J. Phys.: Condens. Matter* **3**, 7443 (1991).

Tables:

Table I

	E(eV)	$^3D_1$(%)	$^3P_1$(%)	$^1P_1$(%)	$d_{5/2}$(%)	$d_{3/2}$(%)
"$^3P_1$"	-5.30	15.35	84.60	0.06	97.8	2.2
"$^3D_1$"	-0.27	82.05	14.50	3.45	60.9	39.1
"$^1P_1$"	15.75	2.61	0.91	96.49	41.3	58.7

Table I: Calculated eigenvalues and eigenstates for the electric-dipole allowed transitions Th $5f^0$ ($^1S_0$) → $5d\,^9 5f^1$ in the presence of spin-orbit interaction. The labels in quotes "$^{2S+1}L_J$" refers to the main character of each state with relative energy E(eV). The percentages give the final state decomposition in LS character ($^3P_1$, $^3D_1$ and $^1P_1$) and in core hole j character ($d_{5/2}$ and $d_{3/2}$). Parameters used in the calculation are $\zeta(5d) = 2.70$ and $\zeta(5f) = 0.21$ eV for the spin-orbit interaction and $F^2 = 7.76$, $F^4 = 4.94$, $G^1 = 9.01$, $G^3 = 5.56$, $G^5 = 3.96$ eV for the 80% reduced $5d,5f$ electrostatic interactions. The spectral intensity of each peak is equal to the amount of $^1P_1$(%) as given in the column.

Table II

	E(eV)	$^3D_1$(%)	$^3P_1$(%)	$^1P_1$(%)	$d_{5/2}$(%)	$d_{3/2}$(%)
"$^3P_1$"	-2.82	0	100	0	80	20
"$^3D_1$"	-0.32	100	0	0	60	40
"$^1P_1$"	15.19	0	0	100	60	40

Table II: Calculated eigenvalues and eigenstates for the electric-dipole allowed transitions Th $5f^0$ ($^1S_0$) → $5d\,^9 5f^1$ in the absence of spin-orbit interaction in the final state. Parameters used in the calculation are same as in Table I, except $\zeta(5d) = 0$ and $\zeta(5f) = 0$. The spectral intensity of each peak is equal to the amount of $^1P_1$(%) as given in the column.

Table III

	E(eV)	$^3D_1$(%)	$^3P_1$(%)	$^1P_1$(%)	$d_{5/2}$(%)	$d_{3/2}$(%)
"$^3P_1$"	-16.49	27.94	71.75	0.31	99.99	0.01
"$^1P_1$"	-15.06	31.97	9.15	58.88	99.99	0.01
"$^1P_1$"	22.51	40.10	19.10	40.81	0.01	99.99

Table III: Calculated eigenvalues and eigenstates for the electric-dipole allowed transitions Th $5f^0$ ($^1S_0$) → $4d^9 5f^1$ for the N_{45} absorption edge. Parameters used in the calculation are $\zeta(4d)$ = 15.38 and $\zeta(5f)$ = 0.23 eV for the spin-orbit interaction and F^2 = 3.54, F^4 = 1.39, G^1 = 0.63, G^3 = 0.67, G^5 = 0.56 eV for the 80% reduced $4d$,$5f$ electrostatic interactions. The spectral intensity of spectral peak is equal to the amount of $^1P_1$(%) as given in the column.

Figure captions:

Figure 1: The $O_{4,5}$ absorption edges for Th, U and Pu metals collected in a TEM (solid gray). The second derivative is calculated for each spectra and overlayed as a black line.

Figure 2: The $O_{4,5}$ absorption edges for UO_2 collected in a TEM (solid gray). The second derivative is calculated for each spectra and overlayed as a black line.

Figure 3: Calculated actinide $O_{4,5}$ absorption spectra with (black thick line) and without (red/grey thin line) 5*d* core spin-orbit interaction for the ground state configurations f^0, f^1, f^2 and f^5. Atomic values of the Hartree-Fock Slater parameters were used as tabulated in Ref. [11]. The relative energy refers to the zero energy of the average of the total final state configuration. The decay channels that give rise to the broadening were not taken into account, instead all spectral lines were broadened with the same Lorentzian line shape of $\Gamma = 0.5$ eV. The pre-peak region and giant resonance are expected to be below and above ~5 eV, respectively.

Figure

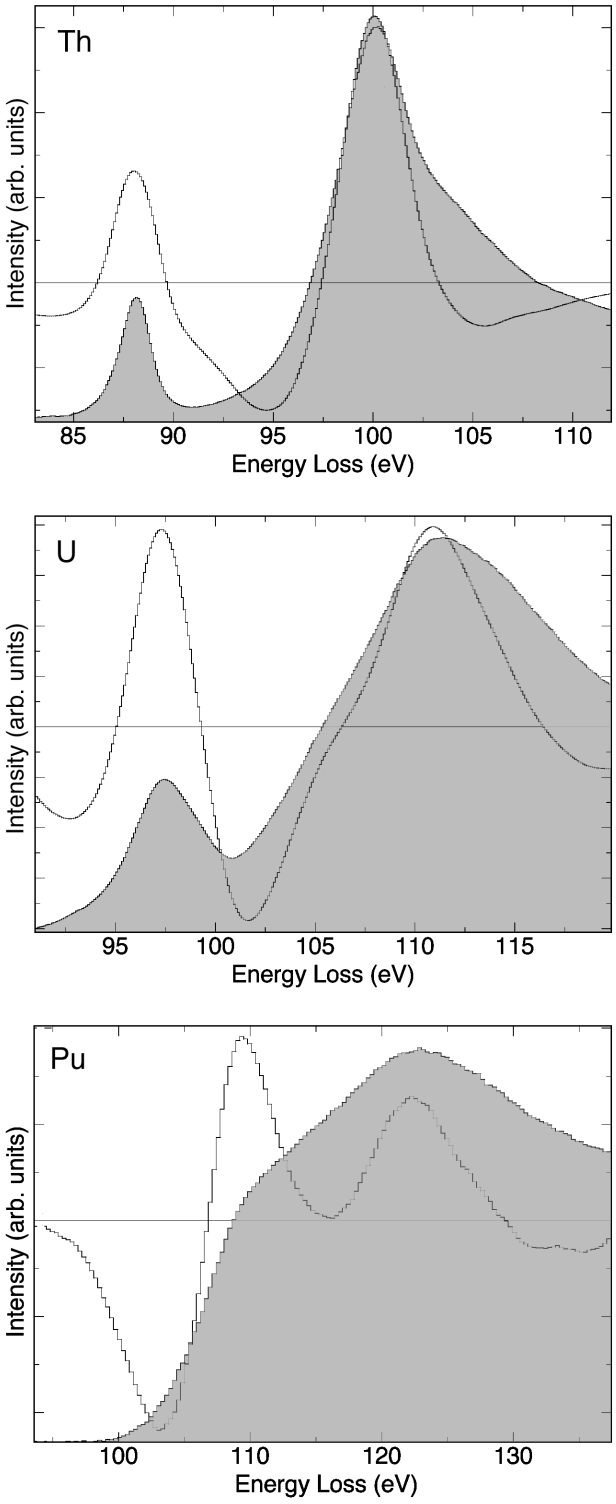

Figure 1

Figure

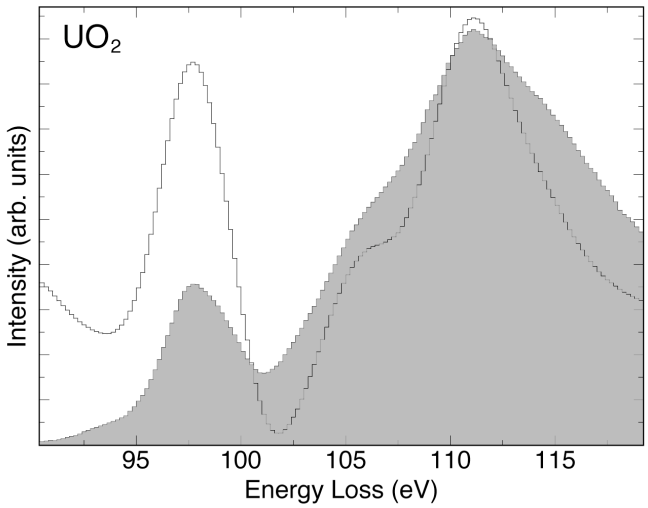

Figure 2

Figure

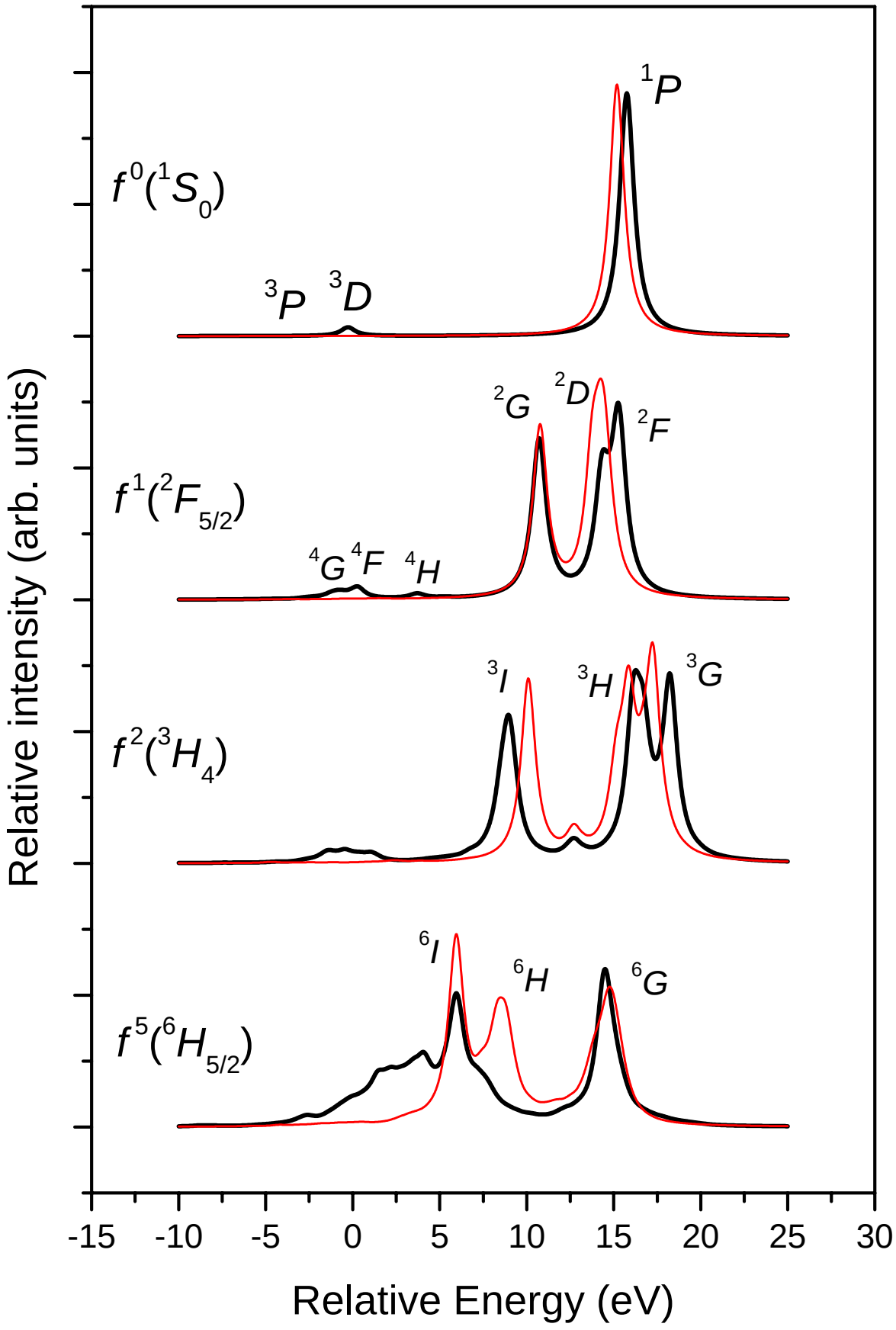
Relative intensity (arb. units)
Relative Energy (eV)
-15
-10
-5
0
5
10
15
20
25
30
$f^0(^1S_0)$
^3P
^3D
^1P
$f^1(^2F_{5/2})$
^4G
^4F
^4H
^2G
^2D
^2F
$f^2(^3H_4)$
^3I
^3H
^3G
$f^5(^6H_{5/2})$
^6I
^6H
^6G